

Ceftriaxone as an Inhibitor for Corrosion of Al in Formic Acid Solutions

Salah Abd El Wanees^{1,2} Mohamed I. Alahmdi¹ Abla Ahmed Hathoot³ Sabry Shaloot²
1.Chemistry Department, Faculty of Science, Tabuk University, Tabuk, Kingdom of Saudi Arabia
2.Chemistry Department, Faculty of Science, Zagazig University, Zagazig 44519, Egypt
3.Department of Chemistry, Faculty of Science, Monufia University, Monufia, Egypt

Abstract

The inhibiting effect of ceftriaxone on the corrosion of Al in HCOOH solution was studied by means of weight loss, thermometry, hydrogen evolution and potentiodynamic polarization techniques, complemented with surface examination using scanning electron microscopy (SEM). The obtained results showed that ceftriaxone are excellent inhibitor in HCOOH solution. The inhibition efficiency increases with inhibitor concentration. Polarization curves indicate that ceftriaxone was acted as a mixed-type inhibitor. The adsorption of the inhibitor on Al surface was found to obey Langmuir isotherm and showed a physisorption mechanism. The thermodynamic activation and adsorption parameters were calculated and discussed.

Keywords: Ceftriaxone, aluminum, corrosion inhibitor, potentiodynamic polarization, adsorption, gravimetry and gasometry

1. INTRODUCTION

The corrosion of Al in acid solutions is considered as a fundamental academic and industrial concern that has received great attention of many scientists. Acid solutions are widely used in industry, the most important fields of application being acid pickling, industrial acid cleaning. On other side, concerns about petroleum depletion, coal and gas, as well as new methods to achieve a more reasonable use of these raw materials to obtain energy have been widely investigated at present, especially some studies about the reduction of greenhouse gases. The hydrogen gas has a very high combustion heat, which is a promising alternative in terms of energy. Recently [1-6], great efforts are focused to produce nascent hydrogen gas by reaction of certain metals with acids. Most research on producing hydrogen is done by the corrosion of Al with mineral acids [1, 2]. Despite the importance of organic acids in industry, few corrosion studies involving these acids have been made. Halides ions was used to increase hydrogen production from corrosion of Al in presence of formic acid solutions [6], and some inorganic salts was used as inhibitors to control hydrogen evolution reaction [6, 7].

Because of the general aggressiveness of acid solutions, inhibitors are commonly used to reduce the corrosive attack on metallic materials [8, 9]. The use of inhibitors is one of the most practical methods of protecting against corrosion, especially for materials in acid media [10]. Numerous studies on corrosion inhibition using organic compounds have been reported [11-24]. It has been accepted that the corrosion inhibition process results from the formation of organic inhibitor films on the metal surface. The inhibitor adsorption mode was strictly dependent on the inhibitor structure [25, 26]. The inhibitor films can be classified as a chemisorbed film, donating a lone pair of electrons attached to a central adsorption atom in a functional group, as an electrostatic adsorption film and as a precipitation and/or a complex film, reacting with dissolved metal ion and organic inhibitor molecule [26]. The choice of the inhibitor was based on the fact that, the compounds contain π -electrons and heteroatoms such as N, O and S, which involve greater adsorption of the inhibitor molecules onto the metal surface.

The aim of the present investigation is to evaluate the efficiency of a pharmaceutical drug, ceftriaxone, as an inhibitor for controlling the corrosion of Al in HCOOH solutions. The inhibition performance is evaluated by gravimetry, gasometry, thermometry and potentiodynamic polarization measurements, complemented with scanning electron microscopy. The adsorption isotherm and mechanism of action of this compound are investigated. The adsorption equilibrium constant and standard free energy of adsorption are calculated.

2. MATERIALS AND METHODS

2.1. Materials Preparation

Aluminium metal with purity of 99.99% provided by the "Aluminium Company of Egypt" was used as the test metal in the present study. Al sheets with dimensions 1.8 cm, 3.7 cm and 0.5 cm were used for weight loss, hydrogen evolution and thermometry measurements. Prior to each experiment, the samples were abraded with 0-, 00- and 000- grit emery papers and then etched for 30 seconds in an alkaline solution of (15 g Na₂CO₃ + 15 g Na₃PO₄) per liter, at 80-85°C. This was followed by rinsing with bi-distilled water and drying. For potentiodynamic polarization measurements, a cylindrical rod of aluminium was prepared as working electrode. The electrode was embedded in Araldite, with exposed cross section surface area of 0.32 cm². Prior to measurements, the surface of the Al electrode was polished with different grades of emery papers, starting with the coarse one and proceeding in steps to the finest (600) grade, using a grinding machine (model Jean Wirtz TG

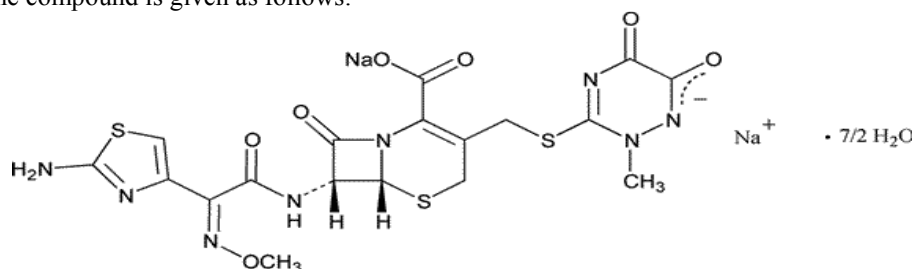
200, Germany). The electrode was then degreased with acetone and finally washed with bi-distilled water, before immersion in the test solution.

2.2. Inhibitors and chemicals.

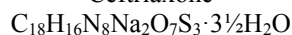
Ceftriaxone is the commercial name of Sodium (6R,7R)-7-[[[(2Z)-2-(2-amino-1,3-thiazol-4-yl)-2-(methoxyimino)acetyl]amino]-3-[[[(2-methyl-5,6-dioxo-1,2,5,6-tetrahydro-1,2,4-triazin-3-yl)sulfanyl]methyl]-8-oxo-5-thia-1-azabicyclo[4.2.0]oct-2-ene-2-carboxylate.

Ceftriaxone is a third-generation cephalosporin antibiotic. It has broad-spectrum activity against Gram positive and Gram-negative bacteria.

The pharmaceutical compound, Ceftriaxone, was manufactured and investigated, by Pharco B International Alexandria, Egypt. The used pharmaceutical drug is chosen because it easily soluble in water, has high molecular weight, and contains many donating atoms (N, S and O). The chemical structure of the compound is given as follows:



Ceftriaxone



Molecular weight = 661.60

All the solutions were prepared using bi-distilled water. The used aggressive solutions were made from 37% HCOOH; appropriate concentrations of acid were prepared using bi-distilled water. 10^{-3} M stock solutions from the investigated inhibitor was prepared by dissolving the appropriate weight of the solid inhibitor in bi-distilled water; the other concentrations of pharmaceutical drug (5×10^{-6} – 1×10^{-3} M) were prepared by dilution with bi-distilled water. All the materials used were of AR grade and used as received.

2.3. Weight Loss Measurements

Weight loss measurements were carried out as described elsewhere [21, 27, 28]. The cleaned degreased Al sheet was weighed before and after immersion in 100 ml of the test solution for the desired period. The average weight loss for each two identical experiments was taken and expressed in $mg\ cm^{-2}$. The weight loss (W) was calculated from the difference between the sample weights before and after immersion in the test solution. The rate of corrosion, v , is expressed in $mg\ cm^{-2}\ min^{-1}$.

2.4. Hydrogen Evolution Measurements

The reaction vessel used for hydrogen evolution reaction and the procedure of determination of corrosion rate of Al in acid solution were the same as described elsewhere [21, 29, 30]. The corrosion rate was assessed from the slope of the linear portions of the volume of hydrogen gas evolved-time plots.

2.5. Thermometry

The reaction vessel and the procedure of thermometric method for following the dissolution of metals in aggressive media have been described previously [21, 31]. The thermometric vessel used is made of Pyrex glass (Mylius tube) kept inside a Dewar's flask to minimize heat exchange with surrounding. The clean Al samples were immersed in 50 ml of the test solution inside the Mylius tube and the variation in temperature was followed with time to $\pm 0.1^\circ C$ using a calibrated thermometer

2.6. Potentiodynamic polarization measurements

Electrochemical measurements were carried out in a conventional three electrode cylindrical glass cell. Platinum electrode was used as a counter electrode, saturated calomel electrode (SCE) as the reference electrode and cylindrical rod of Al was used as the working electrode. Potentiodynamic polarization studies were conducted by using a Potentiostat Wenking (Model POS73- Germany) system. Immersion of the Al electrode in the test solution was allowed until steady state potential is attained, prior to start the polarization measurements. Cathodic and anodic potentiodynamic polarization curves were obtained by using the direct technique at regular intervals. The duration of potential stabilization at each current density value was between 3 and 5 min.

The polarization resistance (R_p) was calculated using the equation [21]:

$$R_P = \frac{\beta_a \beta_c}{2.303 I_{\text{corr}} (\beta_a + \beta_c)} \quad (1)$$

where β_a and β_c are the slopes of the anodic and the cathodic Tafel lines, respectively, and I_{corr} is the corrosion current density.

3. Results and Discussion

3.1. Weight Loss Measurements:

The curves of Figure 1 show the effect of the added pharmaceutical drug, ceftriaxone on the weight loss of Al sheets in 2 M HCOOH solution, as function of the immersion time. From curves of this figure, it is clear that, increasing the concentrations of ceftriaxone causes a marked decrease in the weight loss of Al and consequently, the rate of corrosion is markedly decreased.

Figure 2 shows the variation of the corrosion rate, v , of Al in 2 M HCOOH with the concentration of the inhibitor, C_{inh} . Straight lines are obtained satisfying the relation:

$$v = \alpha - \beta \log C_{\text{inh}} \quad (2)$$

where α and β are constants. The slope β of the straight line is found to be $1.57 \times 10^{-2} \text{ mg cm}^{-2} \text{ min}^{-1}/\text{decade}$, while the constant $\alpha = -1.11 \times 10^{-2} \text{ mg cm}^{-2} \text{ min}^{-1}$, which reflect the tendency of ceftriaxone to act as inhibitor for the corrosion of Al in HCOOH.

The rate of corrosion, v ($\text{mg cm}^{-2} \text{ min}^{-1}$), inhibition efficiency, η , and the surface coverage, θ , are calculated by the following equations [21]:

$$v = \frac{W}{St} \quad (3)$$

$$\eta = \frac{v_0 - v}{v_0} \times 100 \quad (4)$$

$$\theta = \frac{v_0 - v}{v_0} \quad (5)$$

where W is the weight loss of Al sample, S is the total surface area of the specimen, t is the immersion time, v_0 and v are the corrosion rates of Al in the absence and presence of the added inhibitor, respectively. Values of inhibition efficiency, η and surface coverage, θ , calculated at different inhibitor concentrations are listed in Table (1). The presence of the ceftriaxone up to a certain threshold concentration has practically little effect on the rate of corrosion, v , of Al and consequently on the values of θ and η . As the concentration of ceftriaxone is increased, the rate of corrosion decreases and consequently surface coverage, θ , and the percentage inhibition efficiency, η are increased.

3.2. Hydrogen Gas Evolution Measurements:

The dissolution reaction of Al in 2 M HCOOH solutions devoid of- and containing different concentrations of ceftriaxone was studied by using hydrogen evolution measurements. The curves of Figure 3 represent the variation of the volume of H_2 gas in ml/cm^2 with time in the absence and presence of different concentration of ceftriaxone.

Inspection of the curves of Figure 3 reveals that the hydrogen evolution starts after the elapse of a certain time from the immersion of the Al metal in the test solution. This time is identified as the incubation period that is identified as the time needed by the acid to destruct the pre-immersion oxide film and start the dissolution of the bare metal[21]. After this incubation period, the volume of the hydrogen gas evolved increase linearly with time due to the possible simultaneous destruction of the porous film and the continuous dissolution of the bare metal according to the reaction:



The slope of the straight line portions of the curves of Fig 3 is taken as a measure of the rate of corrosion of Al in HCOOH in the absence, v'_0 , and presence of inhibitor, v' . It is noted that, in the presence of increasing concentration of inhibitor, the value of v' is markedly reduced suggesting that the inhibition action of ceftriaxone is concentration dependent.

The inhibition efficiencies, η' and surface coverage, θ of ceftriaxone are calculated from the relations:

$$\eta' = \frac{v'_0 - v'}{v'_0} \times 100 \quad (7)$$

$$\theta = \frac{v'_0 - v}{v'_0} \quad (8)$$

where v and v'_0 are the rates of corrosion in the presence and absence of ceftriaxone, respectively. The values of η' and θ are listed in Table (2).

3. 3. Thermometric Measurements

The effect of addition of ceftriaxone on the variation of the temperature with the immersion time and consequently on the reaction number, N , of dissolution of Al in 4M HCOOH solutions is further investigated. The curves of Figure 4 represent the variation of temperature with time upon the addition of ceftriaxone on Al in 4M HCOOH solutions. As could be seen from this figure, the variation of temperature in the presence of the inhibitor is found to depend on its concentration. Thus, presence of lower concentrations of the inhibitor causes little decrease in the maximum temperature, T_{max} , with a little increase in the time, t , required to reach these maxima. However, on further increase of ceftriaxone concentration, the decrease in the maximum temperature becomes noticeable with marked increase in the time, t . In both cases, the reaction number, N , which is proportional to the rate of corrosion, is always decreases in presence of the inhibitor.

The curves of Figure 5 represent relation between the reaction number, N , and the logarithmic concentration of the inhibitor, C_{inh} . This figure gives rise to a straight line which obeys the relation [21]:

$$N = K - n \log C_{inh} \quad (9)$$

where K and n are constants. The value of n is calculated to be $6.5 \times 10^{-3} \text{ }^\circ\text{C}/\text{min}/\text{decade}$. The value of the constant, $K = 6.95 \times 10^{-3} \text{ }^\circ\text{C}/\text{min}$ represents the rate of corrosion number in presence of 1 M ceftriaxone.

The inhibition efficiency, η'' , is calculated from the relation [21]:

$$\eta'' = 1 - \frac{N_{add}}{N_{free}} \quad (10)$$

where N_{add} and N_{free} are the reaction numbers in the presence and absence of the inhibitor, respectively. The values of the inhibition efficiency, η'' are listed in Table 3. Careful inspection of the curves of Fig 4 and the data of Table 3 reveals that ceftriaxone causes inhibition of the corrosion of Al in 4 M HCOOH, and the inhibition efficiency, η'' , increases with increasing ceftriaxone concentration.

3. 4. Potentiodynamic Polarization Measurements:

The curves of Figure 6 represent the anodic and cathodic potentiodynamic polarization, E -log I curves of Al in 0.5 M HCOOH solutions in the absence and presence of different concentrations of ceftriaxone. Inspection of the curves of Fig 6 reveals that the presence of ceftriaxone causes a decrease in the corrosion rate as evident from the shift of the anodic polarization curves to more positive potentials and the cathodic polarization curves to more negative values. This behavior could be attributed to the adsorption of the inhibitor molecules on the metal surface [21].

The electrochemical corrosion parameters, corrosion potential, E_{corr} , corrosion current density, i_{corr} , anodic Tafel slope, β_a , cathodic Tafel slope, β_c , reciprocal of polarization resistance, R_p^{-1} , surface coverage, θ , and inhibition efficiency, I , are presented in Table 4.

The surface coverage, θ , and the inhibition efficiency, I , are calculated from [21]:

$$\eta'' = 1 - \frac{N_{add}}{N_{free}} \quad (11)$$

$$I = \left(1 - \frac{i_{corr}}{i_{corr}^0} \right) \times 100 \quad (12)$$

where i_{corr} and i_{corr}^0 are the corrosion currents in the presence and absence of ceftriaxone, respectively. Inspection of the curves of Figure 6 reveals the following:

- i) Addition of ceftriaxone causes the shift of E_{corr} to the less negative direction with the marked decrease of the corrosion current density, i_{corr} . This behaviour could be attributed to the suppression of the corrosion reaction.
- ii) The anodic Tafel slope β_a , increase while the cathodic Tafel slope β_c decreases with increasing inhibitor concentration indicating that the inhibitor acted as a mixed type inhibitor [21, 33, 34]. It is assumed to block both the anodic and cathodic sites of the metal surface.
- iii) The values of surface coverage, θ , and inhibition efficiency, I , of ceftriaxone are markedly increased with concentration. This behaviour reflects the inhibition action of this inhibitor.
- iv) The used inhibitor increases the polarization resistance, R_p . The reciprocal of polarization resistance, R_p^{-1} , was taken as a measure of attack [32]. The curves of Figure 7 show the

variation of R_p^{-1} with the inhibitor concentration, which satisfies straight lines according to:

$$R_p^{-1} = K' - n' \log C_{inh} \quad (13)$$

where K' and n' are constants. The value of n' is calculated to be $-3.93 \times 10^{-3} \Omega^{-1} \text{cm}^{-2} \text{decade}^{-1}$. The value of $K' = 8.93 \times 10^{-3} \Omega^{-1} \text{cm}^{-2}$ represents R_p^{-1} in presence of 1M ceftriaxone.

3.5. Scanning electron microscopy

The effect of inhibitor on the corrosion process was examined by SEM investigation of the corroded Al surfaces in 2 M HCOOH in the absence and presence of inhibitor. Figures 8 (A and B) show the images of the surfaces of Al samples after immersion for a period of 3h, in 2M HCOOH in the absence and presence of $1 \times 10^{-3} \text{M}$ inhibitor, respectively. The micrographs show that the surface was strongly damaged in absence of the inhibitor due to the metal dissolution in aggressive solution. In presence of $1 \times 10^{-3} \text{M}$ ceftriaxone, there is a less damage of the Al surface and a good protective film is formed by adsorption of the bulky inhibiting molecules on the metal surface.

3.6. Adsorption isotherm

Adsorption isotherms are very important in determining the mechanism of inhibition. The inhibition of Al corrosion in acidic media in presence of ceftriaxone is attributed to their adsorption on the Al surface and is generally confirmed from the fit of the experimental data to various adsorption isotherms. Several adsorption isotherms are attempted to fit the surface coverage, θ of Al surface including that of Freundlich, Frumkin, Timken and Langmuir isotherms. For the studied inhibitors, it is found that the experimental data obtained from potentiodynamic measurements, as an example, of the other used experimental techniques, could fit the Langmuir adsorption isotherm. According to this isotherm the surface coverage, θ , is related to the inhibitor concentration, C_{inh} by the relation [21, 24]:

$$\frac{\theta}{1-\theta} = \frac{1}{K_{ads}} C_{ads} \quad (14)$$

or

$$\frac{\theta}{1-\theta} = \frac{1}{K_{ads}} C_{ads} \quad (15)$$

where K_{ads} is the adsorption equilibrium constant. Typical plots of C_{ads}/θ vs. C_{ads} for ceftriaxone conferred straight lines as shown in Figure 9. A linear correlation of slope close to unity suggest that adsorption of ceftriaxone obeys Langmuir isotherm.

The values of K_{ads} can be calculated from the intercepts of the straight lines of Figure 9. K_{ads} is related to the standard free energy of reaction, ΔG°_{ads} , in kJ mol^{-1} , with the following equation [21, 24]:

$$K_{ads} = \frac{1}{55.5} \exp\left(\frac{-\Delta G^{\circ}_{ads}}{RT}\right) \quad (16)$$

where 55.5 is the molar concentration of water in the solution, R is the universal gas constant ($8.314 \text{ JK}^{-1} \text{mol}^{-1}$) and T is the absolute temperature. The correlation coefficients, r^2 and the thermodynamic parameters of ceftriaxone, K_{ads} and ΔG°_{ads} , are given in Table (5). In literature it was reported that the high K_{ads} values ($> \sim 100 \text{ M}^{-1}$) attribute to the stronger and more stable adsorbed layer formation on the metal surface [21, 22, 35]. It is clear from Table 5 that, relatively high K_{ads} values reflect the strong adsorption of the used ceftriaxone molecules on Al surface.

Generally, ΔG°_{ads} values around -20 kJ mol^{-1} or lower (more positive) indicate adsorption with electrostatic interaction of the adsorbent and adsorbate which is consistent with physisorption of the inhibitor on the corroded surface. On the other side, ΔG°_{ads} values around or higher (more negative) than 40 kJ mol^{-1} involve charge sharing between the inhibitor molecules and the metal surface (chemisorption) [36-38]. The calculated value of ΔG°_{ads} for ceftriaxone is $-10.16 \text{ kJ mol}^{-1}$. This indicates that the adsorption mechanism of the studied pharmaceutical drug on Al surface is through physisorption.

3.7 Corrosion inhibition mechanism

The inhibition of Al corrosion in HCOOH solutions by the investigated compound is based on the adsorption processes which is readily depend on the adsorption sites in the molecule and their charge density, molecular size and stability of the adsorbed additive in acidic solution. The extent of adsorption of an inhibitor depends on the nature of the metal, the mode of adsorption of the inhibitor and the surface conditions. Adsorption on Al surface is assumed to take place mainly through the active centers attached to the inhibitor and would depend on their charge density. It was concluded that the mode of adsorption depends on the affinity of the metal towards the π -electron clouds of the aromatic ring system and the lone pair of electrons of heteroatoms (N, S and O). Ceftriaxone exhibits excellent inhibition power due to its larger molecular size with presence of different adsorption active sites, that may facilitate better surface coverage.

3. 8. Effect of temperature

The effect of temperature on the inhibitive action of ceftriaxone was performed. The corrosion reaction of Al in 2 M HCOOH solutions devoid of- and containing different concentrations of ceftriaxone was studied at different temperatures by using hydrogen evolution measurements. The change of the corrosion rate with the temperature was calculated in the absence and presence of different concentrations of ceftriaxone, Table 6. It is clear that, in 2 M HCOOH in the absence and presence of inhibitor, the rate of corrosion increases directly with increasing temperature, Fig 10. The variations of the rate of corrosion, r , of Al with the absolute temperature (T) varies according the relation:

$$\log r = \alpha_1 + \beta_1 T \quad (17)$$

where α_1 and β_1 are constants which depend on the solution concentration and metal under test. It is clear that the rate of corrosion increase as the temperature is increased.

The dependence of the corrosion rate, r , on temperature was expressed by the Arrhenius equation [29].

$$r = A \exp(-\Delta E_a/RT) \quad (18)$$

where A is the Arrhenius constant, ΔE_a , is the apparent activation energy, T is the absolute temperature and R is the universal gas constant. Rearranging Eq. (17) gives:

$$\log r = \log A - \Delta E_a/2.303RT \quad (19)$$

The dependence of ($\log r$) on ($1/T$) for Al in 2 M HCOOH in the absence and presence of different concentrations of ceftriaxone are plotted in Fig 11. The activation energies (ΔE_a) are obtained from the slopes of the straight lines, Table 7. The values of (ΔE_a) in the presence of ceftriaxone is higher than in that of free acid. This means that the addition of ceftriaxone to the acid solution increases ΔE_a indicating that the energy barrier for the corrosion reaction increases in presence of ceftriaxone. Many researchers attributed this behaviour to the physorption nature of interaction between inhibitor molecule and the steel surface, while it was found to be opposite in the case with chemical adsorption [39, 40].

The entropy of activation (ΔS^*) and enthalpy of activation (ΔH^*) for the corrosion of Al were calculated from the transition state theory equation [41]:

$$r = (RT/Nh) \exp(\Delta S^*/R) \exp(-\Delta H^*/RT) \quad (20)$$

where h is Planck's constant 6.6261×10^{-34} J.s, N is Avogadro's number 6.0225×10^{23} mol⁻¹, Fig 12 shows the plots of $\log(r/T)$ versus ($1/T$) for blank and ceftriaxone. From the slope ($-\Delta H^*/2.303R$) and intercept [$\log(R/Nh) + (\Delta S^*/2.303R)$] of the straight lines ΔH^* and ΔS^* , respectively were obtained. The calculated values are shown in Table 6. The positive sign of the enthalpy, ΔH^* , denotes that the transition state (the activated complex) is endothermic nature [9]. The values of entropy of activation (ΔS^*) in the absence and presence of inhibitor are negative. This indicates that the activated complex in the rate-determining step represents an association rather than dissociation meaning that a decrease in disordering takes place on going from reactants to activated complex [42].

REFERENCES

- [1] Soler L., Candela A.M., Macanás J., Muñoz M., Casado J., (2009) *Int. J. Hydrogen Energy*, 34: 8511-8518.
- [2] Lædre S., Kongstein O.E., Oedegaard A., Seland F., Karoliussen H., (2012) *Int. J. Hydrogen Energy*, 37: 18537-18546.
- [3] Soler L., Candela A.M., Macanás J., Muñoz M., Casado J., (2009) *J. Power Sources* 192:21-26.
- [4] Macanás J., Soler L., Candela A.M., Muñoz M., Casado J., (2011) *Energy*, 36 : 2493-2501.
- [5] Czech E., Troczynski T., (2010) *Int. J. Hydrogen Energy*, 35: 1029-1037.
- [6] Deyab M.A., (2013) *J. Power Sources*, 242: 86-90.
- [7] Deyab M.A., Keera S.T., El Sabagh S. M, (2013) *Corros. Sci.* 53: 2592–2597.
- [8] Abd El Aal E.E., Abd El Wanees S., Farouk A., Abd El Haleem S.M., (2013) *Corros. Sci.* 68: 14-24.
- [9] Hegazy M.A., Badawi A.M., Abd El Rehim S.S., Kamel W.M., (2013) *Corros. Sci.* 69: 110–122.
- [10] Singh A.K. (2012) *Ind. Eng. Chem. Res.* 51: 3215–3223.
- [11] Ahmed, A. Farag, Hegazy M. A., (2013) *Corros. Sci.*, 74: 168–177.
- [12] Pournazari Sh., Moayed M.H., Rahimizadeh M., (2013) *Corros. Sci.* 76: 20–31.
- [13] Zhang Q.B., Hua Y. X., (2009) *Electrochim. Acta* 54: 1881–1887.
- [14] Emregul K.C., Hayval M., (2004) *Mater. Chem. Phys.* 83: 209-215.
- [15] Quartarone G., Ronchin L., Vavasori A., Tortato C., Bonaldo L., (2012) *Corros. Sci.* 64: 82–89.
- [16] Hosseini S. M. A., Azimi A., (2009) *Corros. Sci.* 51: 728-735.
- [17] Fouda A.S., Eldesoky M. A., Elmorsi Fayed T.A.; Atia M. F., (2013) *Int. J. Electrochem. Sci.* 8: 10219 – 10238.
- [18] Hegazy M.A., Ahmed H. M., El-Tabei A.S., (2011) *Corros. Sci.* 53: 671–678.
- [19] Qian B., Wang J., Zheng M., Hou B., (2013) *Corros. Sci.* 75: 184–192.
- [20] Hernandez-Espejel A., Dominguez-Crespo M.A., Cabrera-Sierra, R. Rodriguez-Meneses C., Arce-Estrada, E.M., (2010) *Corros. Sci.* 52: 2258–2267.

- [21] Abd El Haleem, S.M.; Abd El Wanees, S.; Abd El Aal, E.E., Farouk A., (2013) *Corros. Sci.* 68: 1-13.
[22] Safak S., Duran B., Yurt A., Turkoglu G., (2012) *Corros. Sci.*, 54: 251-259.
[23] Ahamad I., Prasad R., Quraishi M. A., (2010) *Mater. Chem. Phys.* 124:1155-1165.
[24] Abdallah M., Zaafarany I., Al-Karane S. O., Abd El Fattah A. A., (2012) *Arabian J. of Chemistry* 5: 225-234.
[25] El Achouri M., Infante M. R., Izquierdo F., Kertit, S., Gouttoya H.M., Nciri B., (2001) *Corros. Sci.* 43: 19-35.
[26] Li, X., Deng, S., Fu H., (2010) *Corros. Sci.* 52: 3413-3420.
[27] S.M. Hassan, Y.A Elawady, A.I Ahmed, A.O. Baghlaf, (1979) *Corros. Sci.* 19: 951-959.
[28] Oguzie, E. E.; Njoku, V.O., Enenebeaku, C. K., Akalezi, C.O., Obi C., (2008) *Corros. Sci.* 50: 3480-3486.
[29] Abdel-Gaber A. M., Khamis, E., Abo-Eldahab Adeel H. Sh., (2010) *Mater. Chem. Phys.* 124: 773-779.
[30] Solomon M. M., Umoren S. A., Udosoro I. I., Udoh A.P., (2010) *Corros. Sci.* 52: 1317-1325.
[31] Abd El Haleem, S. M., Abd El Aal, E.E., (2008) *J. Mater. Process. Tech* 204: 139-146.
[32] Mahgoub F. M., Abd El Nabey B. A., El-Samady Y. A., (2010) *Mater. Chem. Phys.* 120: 104-108.
[33] Oguize E. E., (2007) *Corros. Sci.* 49: 1527-1539.
[34] Shen C. B., Wang S. G., Yang H.Y., Long K., Wang F. H., (2006) *Appl. Surf. Sci.* 253: 2118-2122.
[35] Lagrenee M., Mernari B., Bouanis M., Traisnel M., Bentiss F., (2002) *Corros. Sci.* 44: 573-588.
[36] Zhang Q., Hua Y., (2010) *Mater. Chem. Phys.* 119: 57-64.
[37] Khaled K. F., (2010) *Corros. Sci.* 52: 2905-2916.
[38] Biligic S., Shain M., (2001) *Mater. Chem. Phys.* 70: 290-295.
[39] Umoren S.A., Obot I. B., Obi-Egbedi N. O., (2009) *J. Mater. Sci.* 44: 274-279.
[40] Avci G. (2008) *Colloids Surf A: Physicochemical and Engineering Aspects* 317: 730-736.
[41] Bouklah M., Benchat N., Hammouti B., Aouniti A., Kertit S., (2006) *Mater. Lett.* 60: 1901-1905
[42] Fouda A.S., Heikal F.E., Radwan M.S., (2009) *J. Appl. Electrochem* 39: 391-402.

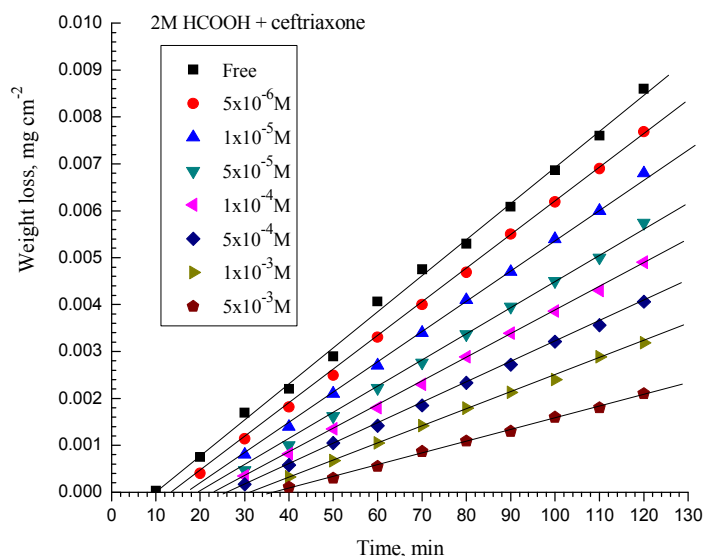


Fig 1. Variation of the volume of hydrogen evolved on Al in 2 M HCOOH in the absence and presence of different concentrations of ceftriaxone.

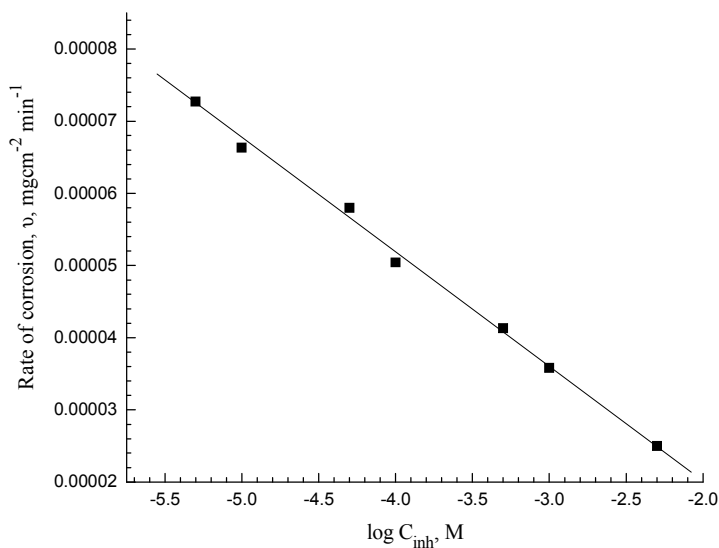


Fig 2. Variation of the rate of corrosion with the logarithm of the inhibitor concentration.

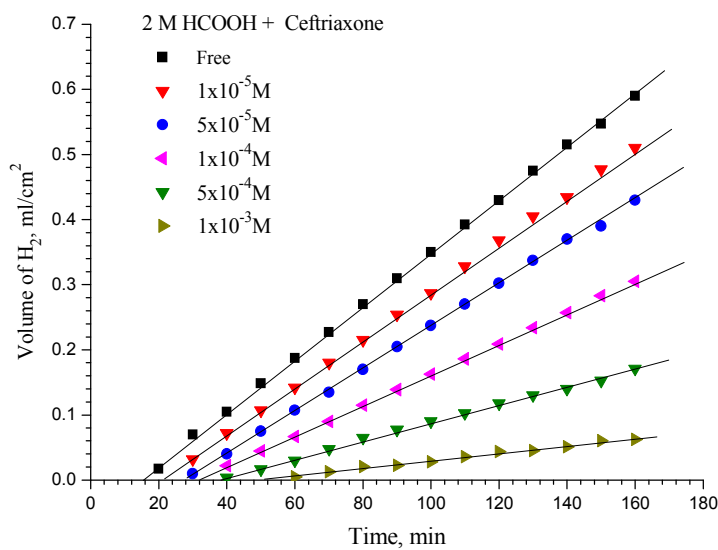


Fig 3. Variation of the volume of hydrogen gas evolved on Al in 2 M HCOOH in the absence and presence of different concentrations of ceftriaxone.

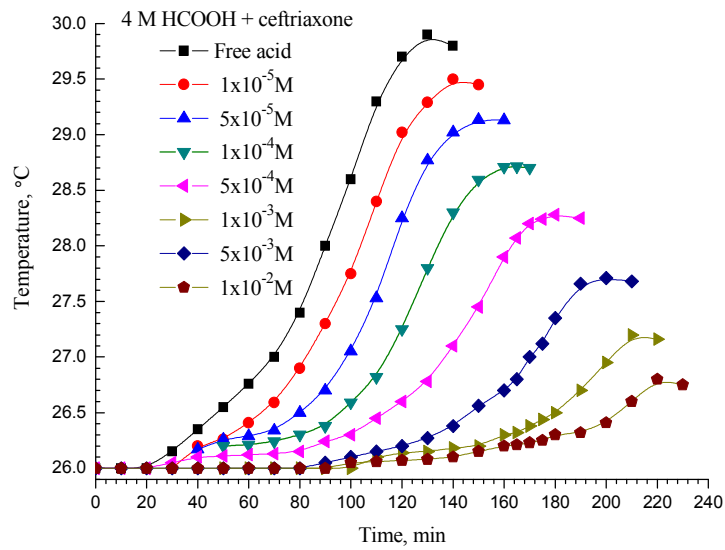


Fig 4. Variation of the temperature with the immersion time of Al immersed in 4MHCOOH in the absence and presence of different concentrations of ceftriaxone.

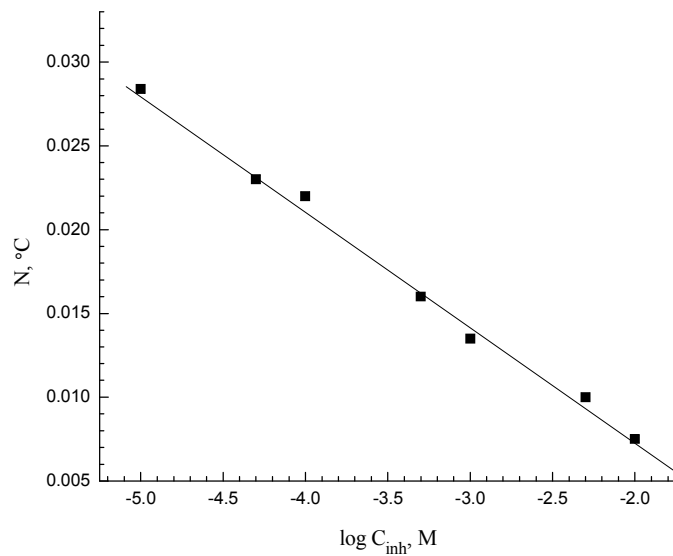


Fig 5. Variation of the reaction number, N , as function of the logarithm of the ceftriaxone concentration, C_{inh} .

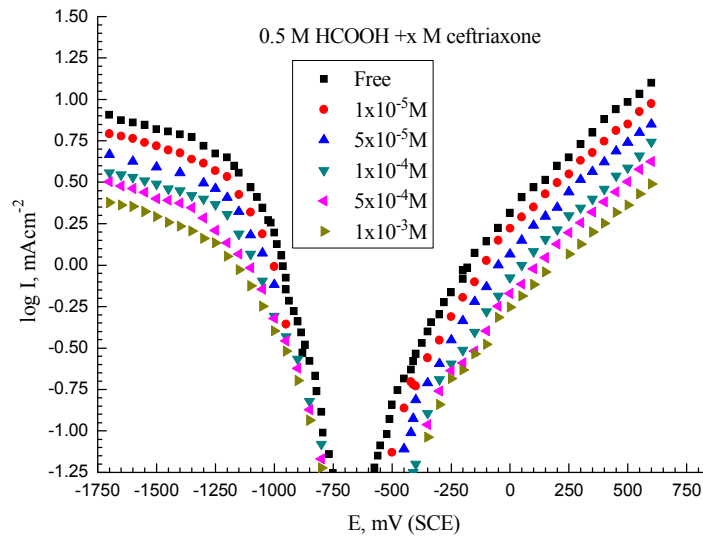


Fig 6. Potentiodynamic polarization curves of Al in 0.5 M HCOOH in the absence and presence of different concentrations of ceftriaxone.

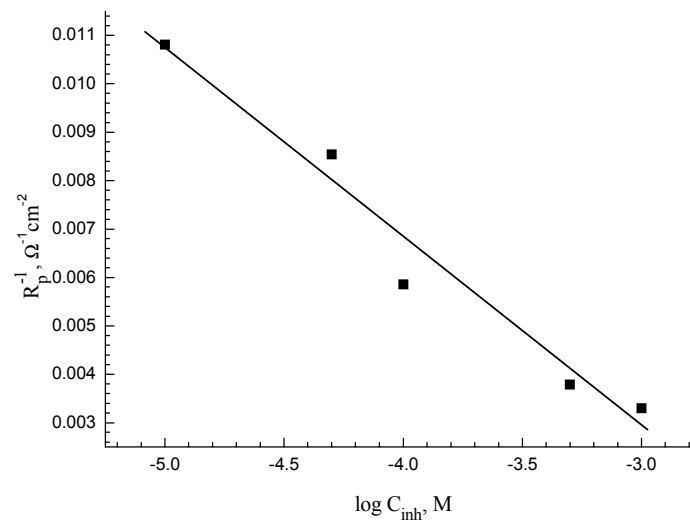


Fig 7. Variation of the reciprocal of polarization resistance, $1/R_p$, versus the logarithm of the inhibitor concentration, C_{inh} .

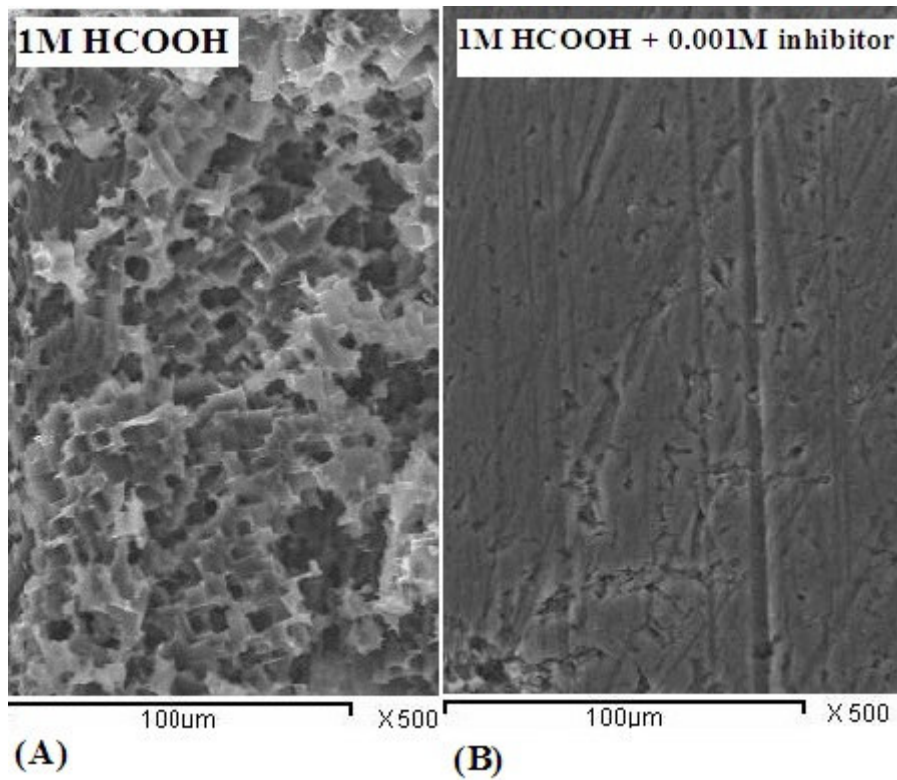


Fig 8. SEM micrographs of Al electrode surfaces immersed for a period of 3 hr in (A) 2M formic acid and (B) 2M formic acid + 10^{-3} M ceftriaxone.

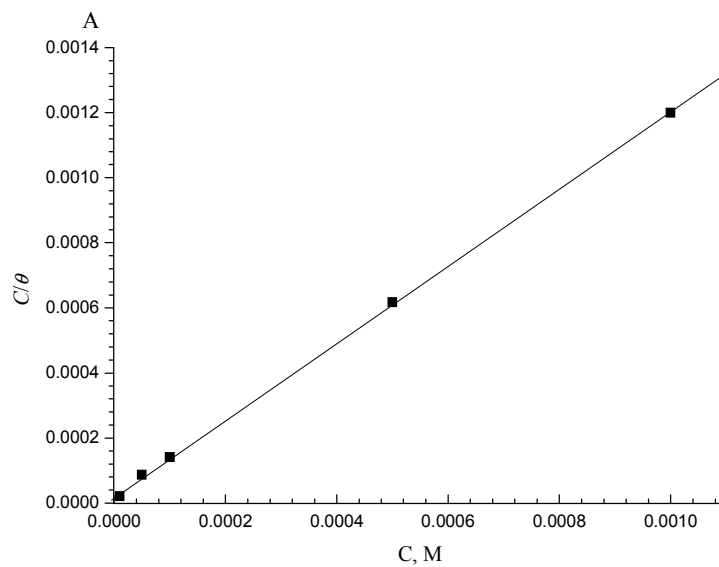


Fig 9. Langmuir's adsorption isotherm for ceftriaxone in 2 M HCOOH.

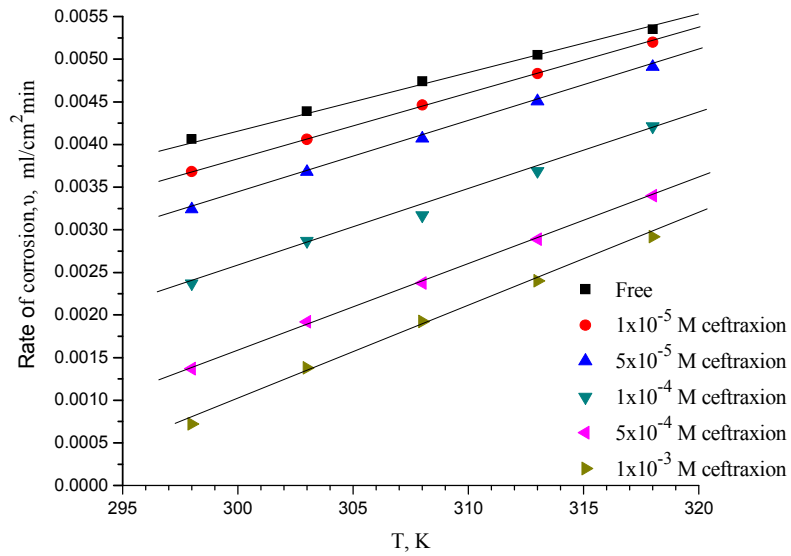


Fig 10. Variations of the rate of corrosion of Al with the absolute temperature.

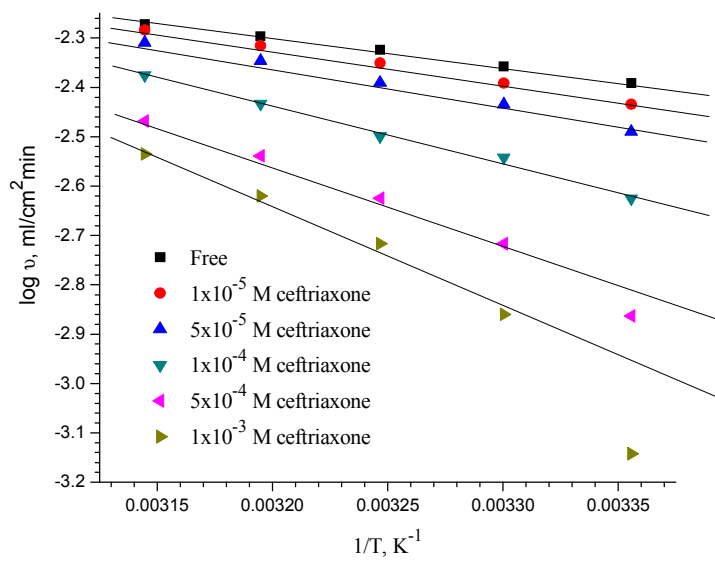


Fig 11. Variation of ($\log r$) with ($1/T$) for Al in 2 M HCOOH in the absence and presence of different concentrations of ceftriaxone

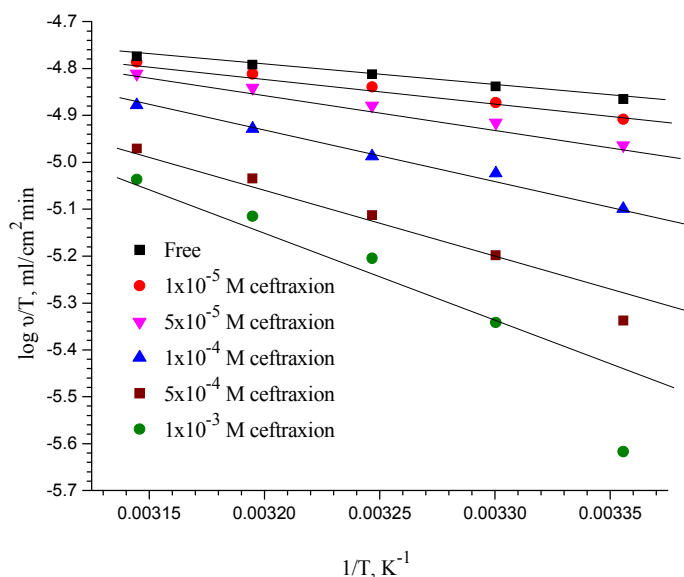


Fig 12. The plots of $\log (r/T)$ versus $(1/T)$ for Al in 2 M HCOOH in the absence and presence of different concentrations of ceftriaxone.

TABLE 1. Corrosion parameters of Al in 2 M HCOOH in the absence and presence of different concentrations of ceftriaxone (data obtained from weight loss measurements).

Concentration, M	v , $\mu\text{g cm}^{-2}\text{min}^{-1}$	η	θ
Blank	7.67×10^{-2}	----	----
$5 \times 10^{-6}\text{M}$	7.27×10^{-2}	05.2	0.052
$1 \times 10^{-5}\text{M}$	6.63×10^{-2}	13.5	0.135
$5 \times 10^{-5}\text{M}$	5.80×10^{-2}	24.3	0.243
$1 \times 10^{-4}\text{M}$	5.04×10^{-2}	34.3	0.343
$5 \times 10^{-4}\text{M}$	4.31×10^{-2}	43.4	0.434
$1 \times 10^{-3}\text{M}$	3.58×10^{-2}	53.3	0.533
$5 \times 10^{-3}\text{M}$	2.50×10^{-2}	67.3	0.673

TABLE 2. Corrosion parameters of Al in 2 M HCOOH without and with different concentrations ceftriaxone (obtained from gasometry measurements).

Concentration, M	v , $\text{ml cm}^{-2}\text{min}^{-1}$	η' %	θ
Blank	40.6×10^{-4}	-	-
$1 \times 10^{-5}\text{M}$	36.8×10^{-4}	8.90	0.089
$5 \times 10^{-5}\text{M}$	32.4×10^{-4}	19.8	0.198
$1 \times 10^{-4}\text{M}$	23.7×10^{-4}	41.3	0.413
$5 \times 10^{-4}\text{M}$	13.7×10^{-4}	66.1	0.661
$1 \times 10^{-3}\text{M}$	05.7×10^{-4}	85.9	0.859

TABLE 3. Variation of the reaction number, N and the inhibition efficiency, η'' with ceftriaxone concentration.

Concentration, M	N , $^{\circ}\text{C min}^{-1}$	η''
$1 \times 10^{-5}\text{M}$	0.025	16.67
$5 \times 10^{-5}\text{M}$	0.021	30.51
$1 \times 10^{-4}\text{M}$	0.015	49.59
$5 \times 10^{-4}\text{M}$	0.013	57.63
$1 \times 10^{-3}\text{M}$	0.008	71.83
$5 \times 10^{-3}\text{M}$	0.006	81.37
$1 \times 10^{-2}\text{M}$	0.004	88.09

TABLE 4. The electrochemical corrosion parameters of Al in 0.5M HCOOH upon additions of different concentrations of ceftriaxone.

Concentration, M	$-E_{\text{corr}}, V_{\text{SCE}}$	$I_{\text{corr}}, \text{mA/cm}^2$	$\beta_a, \text{mV/decade}$	$-B_c, \text{mV/decade}$	θ	η	$R_p^{-1}, \Omega^{-1}\text{cm}^{-2} \times 10^3$
Blank	0.693	0.660	149	145	----	----	20.68
$1 \times 10^{-5}\text{M}$	0.692	0.352	151	149	0.47	46.7	10.80
$5 \times 10^{-5}\text{M}$	0.691	0.280	152	150	0.58	57.6	8.50
$1 \times 10^{-4}\text{M}$	0.690	0.190	151	148	0.71	71.2	5.85
$5 \times 10^{-4}\text{M}$	0.589	0.125	153	151	0.81	81.1	3.79
$1 \times 10^{-3}\text{M}$	0.588	0.110	155	152	0.83	83.3	3.30

Table 5. The correlation coefficients, r^2 , adsorption equilibrium constant K_{ads} , and standard free energy of reaction, $\Delta G^{\circ}_{\text{ads}}$, of adsorption ceftriaxone on Al in 0.5M HCOOH.

r^2	$K_{\text{ads}}, \text{mol}^{-1}$	$-\Delta G^{\circ}_{\text{ads}}, \text{kJ/mol}$
0.998	48544	10.16

TABLE 6. Variation of the corrosion rate of Al in 2M HCOOH in the absence and presence of different concentrations of ceftriaxone with temperature.

Temperature, K	Rate of corrosion, $\text{ml/cm}^2\text{min}$					
	Free	$1 \times 10^{-5}\text{M}$	$5 \times 10^{-5}\text{M}$	$1 \times 10^{-4}\text{M}$	$5 \times 10^{-4}\text{M}$	$1 \times 10^{-3}\text{M}$
298	0.00406	0.00368	0.0024	0.00237	0.00137	0.00072
303	0.00439	0.00406	0.00368	0.00287	0.00192	0.00138
308	0.00474	0.00446	0.00407	0.00317	0.00237	0.00192
313	0.00505	0.00483	0.00451	0.00369	0.00289	0.00253
318	0.00535	0.00520	0.00491	0.00421	0.00340	0.00331

TABLE 7. The correlation coefficients, r^2 , and activation parameters for corrosion of Al in 2M HCOOH in the absence and presence of different concentrations of ceftriaxone.

Concentration	r^2	$\Delta E_a, \text{kJ/mol}$	$\Delta H^*, \text{kJ/mol}$	$-\Delta S^*, \text{J/mol}$
Blank	0.994	10.91	8.34	262
$1 \times 10^{-5}\text{M}$	0.996	13.71	11.08	254
$5 \times 10^{-5}\text{M}$	0.994	16.31	13.76	246
$1 \times 10^{-4}\text{M}$	0.988	22.07	19.50	229
$5 \times 10^{-4}\text{M}$	0.996	30.63	28.05	204
$1 \times 10^{-3}\text{M}$	0.978	39.63	37.07	177